Inorg. Chem. **2006**, *45*, 8638–8647

Syntheses, Structures, and Nonlinear Optical Properties of Heteroselenometallic W–Se–Ag Cluster Compounds Containing Phosphine Ligands

Qian-Feng Zhang,*,† Jihai Ding,† Zhan Yu,† Yinglin Song,‡ Alexander Rothenberger,§ Dieter Fenske,§ and Wa-Hung Leung||

Department of Applied Chemistry, Anhui University of Technology, Ma'anshan, Anhui 243002, P. R. China, Department of Chemistry, The Hong Kong University of Science and Technology, Clear Water Bay, Kowloon, Hong Kong, P. R. China, Institut für Anorganische Chemie, Universität Karlsruhe (TH), 76128 Karlsruhe, Germany, and Department of Physics, Harbin Institute of Technology, Harbin 150001, P. R. China

Received June 16, 2006

Treatment of $[Et_4N]_2[WSe_4]$ with a 1:1 mixture of $AgNO_3$ and PCy_3 (Cy = cyclohexyl) in the absence of iodide afforded a linear trinuclear compound $[(\mu\text{-}WSe_4)(AgPCy_3)_2]$ (**1**). A similar reaction in the presence of iodide gave rise to the isolation of the cubanelike compound $[(\mu_3\text{-}WSe_4)Ag_3(PCy_3)_3(\mu_3\text{-}I)]$ (**2**). Treatment of $[Et_4N]_2[WSe_4]$ with AgI in the presence of bidentate phosphine ligands bis(diphenylphosphino)amine (dppa) and bis(diphenylphosphino)-methane (dppm) afforded the tetranuclear compounds $[(\mu_3\text{-}WSe_4)Ag_3(\mu\text{-}I)(\mu\text{-}dppa)_2]$ (**3**) and $[(\mu_3\text{-}WSe_4)Ag_3(\mu_3\text{-}I)(\mu\text{-}dppm)_2]$ (**4**), respectively, which exhibit an open butterfly configuration. A novel hexanuclear cluster compound $[(\mu_3\text{-}WSe_4)_2Ag_4(\mu\text{-}dppm)_3]$ (**5**) was obtained from interaction of $[Et_4N]_2[WSe_4]$ with $AgNO_3$ and dppm in the absence of iodide source. The above cluster compounds are electrically neutral and air-stable in both solution and the solid state and have been characterized by electronic, infrared, mass, and NMR spectroscopies. The solid-state structures of five cluster compounds have been established by X-ray crystallography. The nonlinear optical properties of compounds **4** and **5** were examined by *z*-scan techniques with 7 ns pulses at 532 nm. The optical limiting effects of compounds **1**, **2**, **4**, and **5** were determined and compared with related argentoselenometallic compounds.

Introduction

While the chemistry of coinage-metal compounds containing the $[MS_4]^{2-}$ (M = Mo, W) anions has been well developed,[1] analogous compounds with the $[MSe_4]^{2-}$ anions has received comparatively less attention.[2] Ibers and one of us have studied the interactions of $[MSe_4]^{2-}$ anions with a series of coinage-metal cations and isolated a number of MSe_4 compounds with various structural types including linear, butterfly, cubane, incomplete-cubane, coplanar T-frame and open cross-frame, cage, and pinwheel shapes.[3−10] Two

* To whom correspondence should be addressed. E-mail: zhangqf@ahut.edu.cn.
† Anhui University of Technology.
‡ Harbin Institute of Technology.
§ Universität Karlsruhe (TH).
|| The Hong Kong University of Science and Technology.

(1) (a) Müller, A.; Diemann, E.; Jostes, R.; Bögge, H. *Angew. Chem., Int. Ed. Engl*. **1981**, *20*, 934. (b) Wu, X. T.; Chen, P. C.; Du, S. W.; Zhu, N. Y.; Lu, J. X. *J. Cluster Sci*. **1994**, *5*, 265. (c) Hou, H. W.; Xin X. Q.; Shi, S. *Coord. Chem. Rev*. **1996**, *153*, 169. (d) Niu, Y. Y.; Zheng, H. G.; Hou, H. W.; Xin, X. Q. *Coord. Chem. Rev*. **2004**, *248*, 169.

(2) (a) Ansari, M. A.; Ibers, J. A. *Coord. Chem. Rev*. **1990**, *100*, 233. (b) Roof, L. C.; Kolis, J. W. *Chem.* Rev. **1993**, *93*, 1037. (c) Zhang, Q. F.; Leung, W. H.; Xin, X. Q. *Coord. Chem. Rev*. **2002**, *224*, 35.

(3) (a) Christuk, C. C.; Ansari, M. A.; Ibers, J. A. *Inorg. Chem*. **1992**, *31*, 4365. (b) Christuk, C. C.; Ibers, J. A. *Inorg. Chem*. **1993**, *37*, 5105. (c) Salm, R. J.; Ibers, J. A. *Inorg. Chem*. **1994**, *33*, 4216. (d) Salm, R. J.; Misetic, A.; Ibers, J. A. *Inorg. Chim. Acta* **1995**, *240*, 239.

(4) (a) Zhang, Q. F.; Cao, R.; Hong, M. C.; Wu, D. X.; Zhang, W. J.; Zheng, Y.; Liu, H. Q. *Inorg. Chim. Acta* **1998**, *271*, 93. (b) Zhang, Q. F.; Leung, W. H.; Song, Y. L.; Hong, M. C.; Kennard, C. L.; Xin, X. Q. *New J. Chem.* **2001**, *25*, 465.

(5) Wang, Q. M.; Wu, X. T.; Huang, Q.; Sheng T. L.; Lin, P. *Polyhedron* **1997**, *16*, 1439.

(6) (a) Ansari, M. A.; Bollinger, J. C.; Christuk, C. C.; Ibers, J. A. *Acta Crystallogr*. **1994**, *C50*, 869. (b) Du, S. W.; Wu, X. T.; Lu, J. X. *Polyhedron* **1994**, *12*, 841.

(7) (a) Zhang, Q. F.; Hong, M. C.; Su, W. P.; Cao, R.; Liu, H. Q. *Polyhedron* **1997**, *16*, 1433. (b) Zhang, Q. F.; Hong, M. C.; Liu, H. Q. *Transition Met. Chem*. **1997**, *22*, 156. (c) Zhang, Q. F.; Xin, X. Q.; Hong, M. C.; Cao, R.; Raj, S. S. S.; Fun, H. K. *Acta Crystallogr*. **1999**, *C55*, 726. (d) Zhang, Q. F.; Zhang, C.; Song, Y. L.; Xin, X. Q. *J. Mol. Struct.* **2000**, *525*, 79. (e) Yao, W. R.; Song, Y. L.; Xin, X. Q.; Zhang, Q. F. *J. Mol. Struct.* **2003**, *655*, 391.

10.1021/ic0610839 CCC: $33.50
Published on Web 09/22/2006

polymeric heterometallic clusters containing the $[WSe_4]^{2-}$ core have also been synthesized by both solution and solid-state methods.[11] Among all heteroselenometallic cluster compounds isolated thus far, the most extensively explored system is the Cu(I)/$[MSe_4]^{2-}$ clusters. Compared with the Cu congeners, relatively few argentoselenometallic clusters have been synthesized. Examples of structurally characterized argentoselenometalles include trinuclear linear $[(\mu\text{-}WSe_4)(AgPPh_3)_2]$[12] and $[(\mu\text{-}WSe_4)(AgPPh_3)\{Ag(PPh_3)_2\}]$,[4b] incomplete cubic $[(\mu\text{-}WSe_4)(AgPPh_3)_2(\mu\text{-}C_5H_5NS)]$,[5] cubanelike $[(\mu_3\text{-}MSe_4)(AgPR_3)_3(\mu_3\text{-}X)]$ (M = Mo, W; R_3 = Ph_3, $PhMe_2$; X = Cl, Br, I),[6,7] and one-dimensional helical polymeric $\{[La(Me_2SO)_8][(\mu_3\text{-}WSe_4)_3Ag_3]\}_n$.[11] The difficulty in the synthesis of argentoselenometallic clusters is probably due to the low solubility of Ag(I) species that are involved in the self-assembly with the $[MSe_4]^{2-}$ anion. To overcome this problem, organic phosphine ligands are used to increase the solubility of the Ag(I) species and facilitate their cluster buildup reactions with the $[MSe_4]^{2-}$ anion in organic solvents.

This study details the synthesis and characterization of five new selenometallic clusters containing univalent silver(I) ion and phosphine ligands. The goal of this work is to develop rational synthetic routes to selenometallic clusters with core structures that are complementary to those reported in the literature.[3−12] Our interest in argentoselenometallic clusters is originated from their potential applications as third-order nonlinear optical (NLO) materials.[13] Previous studies on the effect of atomic skeleton atoms on the NLO properties revealed that both the photostability and optical limiting effects are greatly improved upon replacing Cu(I) with Ag(I) ions in heteroselenometallic clusters. Thus, argentoselenometalatic cluster compounds appear to be the most promising candidates of optical limiting materials among all the selenometallic cluster compounds studied so far.[4b,13] The NLO data for the newly prepared argentoselenometallic clusters reported in this work provide further support for this speculation.

Experimental Section

Materials. All syntheses were performed in oven-dried glassware under a purified nitrogen atmosphere using standard Schlenk techniques. The solvents were purified by conventional methods and degassed prior to use. $[Et_4N]_2[WSe_4]$ was prepared by a modification of the literature method.[14] AgI, $AgNO_3$, PCy_3 (Cy = cyclohexyl), and bis(diphenylphosphino)methane (dppm) were purchased from Aldrich Ltd. and used without further purification. Bis(diphenylphosphino)amine (dppa) was synthesized from the reaction of Ph_2PCl and $(Me_3Si)NH(SiMe_3)$ in toluene.[15]

Instrumentation. All elemental analyses were carried out using a Perkin-Elmer 2400 CHN analyzer. Electronic absorption spectra were obtained on a Shimadzu UV-3000 spectrophotometer. Infrared spectra were recorded on a Digilab FTS-40 spectrophotometer with use of pressed KBr pellets, and positive FAB mass spectra were recorded on a Finnigan TSQ 7000 spectrometer. NMR spectra were recorded on a Bruker ALX 300 spectrometer operating at 300 and 121.5 MHz for ^{1}H and ^{31}P, respectively, and chemical shift (δ, ppm) were reported with reference to $SiMe_4$ (^{1}H) and H_3PO_4 (^{31}P). The ^{77}Se NMR spectra were recorded on a Varian Unity-500 spectrometer equipped with a tunable probe and a deuterium lock. The chemical shifts were referenced to an external standard PhSeSePh at δ = 460 ppm.

Synthesis of $[(\mu\text{-}WSe_4)(AgPCy_3)_2]$ (1). To a solution of $[Et_4N]_2[WSe_4]$ (150 mg, 0.20 mmol) in DMF (5 mL) was added a mixture of $AgNO_3$ (68 mg, 0.40 mmol) and PCy_3 (112 mg, 0.40 mmol) in CH_2Cl_2 (15 mL). After the reaction mixture had been stirred for 2 h at room temperature, it was filtered through a filter paper to provide an orange filtrate. The filtrate was carefully layered with Et_2O, and the orange-red crystals of **1** were collected after 1 week. Yield: 132 mg (53%). Anal. Calcd for $C_{36}H_{66}P_2Ag_2Se_4W$: C, 33.9; H, 5.21. Found: C, 33.8; H, 5.19. UV−vis (CH_2Cl_2, λ_{max}/nm, $10^{-3}\epsilon$/$M^{-1}\cdot cm^{-1}$): 310 (8.32), 453 (2.77). IR (KBr, cm^{-1}): ν(W−Se), 301 (m). ^{1}H NMR ($CDCl_3$, ppm): δ 1.22−2.14 (m, C_6H_{11}). ^{31}P NMR ($CDCl_3$, ppm): δ 55.4. ^{77}Se NMR ($CDCl_3$, ppm): δ 1135. MS (FAB): m/z 1277 ($M^+ + 1$).

Synthesis of $[(\mu_3\text{-}WSe_4)Ag_3(PCy_3)_3(\mu_3\text{-}I)]$ (2). To a solution of $[Et_4N]_2[WSe_4]$ (150 mg, 0.20 mmol) in DMF (5 mL) was added a mixture of $AgNO_3$ (68 mg, 0.40 mmol) and PCy_3 (112 mg, 0.40 mmol) in CH_2Cl_2 (15 mL). After the reaction had been stirred for 15 min at room temperature, the solid $[Et_4N]I$ (52 mg, 0.20 mmol) was added. After the mixture was continuously stirred for 1 h, it was filtered through a filter paper to provide a clearly orange filtrate. The filtrate was carefully layered with THF/Et_2O (v/v: 1:1), and after 1 week the orange-red crystals of **2** were obtained. Yield: 216 mg (62%). Anal. Calcd for $C_{54}H_{99}P_3IAg_3Se_4W$: C, 36.2; H, 5.57. Found: C, 36.1; H, 5.54. UV−vis (CH_2Cl_2, λ_{max}/nm, $10^{-3}\epsilon$/$M^{-1}\cdot cm^{-1}$): 311 (7.84), 456(2.63), 514 (sh). IR (KBr, cm^{-1}): ν(W−Se), 313 (s), 296 (m). ^{1}H NMR ($CDCl_3$, ppm): δ 1.26−2.18 (m, C_6H_{11}). ^{31}P NMR ($CDCl_3$, ppm): δ 44.8. ^{77}Se NMR ($CDCl_3$, ppm): δ 1664, 1058. MS (FAB): m/z 1792 ($M^+ + 1$).

Synthesis of $[(\mu_3\text{-}WSe_4)Ag_3(\mu\text{-}I)(\mu\text{-dppa})_2]\cdot$dmf (3·dmf). To a solution of $[Et_4N]_2[WSe_4]$ (150 mg, 0.20 mmol) in DMF (5 mL) was added a mixture of AgI (118 mg, 0.50 mmol) and dppa (118 mg, 0.30 mmol) in CH_2Cl_2 (15 mL). After the reaction had been stirred for 10 min at room temperature, it was filtered through a filter paper to provide an orange red filtrate. Slow addition of a mixture solvent of THF/Et_2O (1:4) resulted in the formation of red block crystals suitable for a single-crystal X-ray diffraction analysis, which were identified as **3**·dmf. Yield: 166 mg (52%). Anal. Calcd for $C_{48}H_{42}N_2P_4IAg_3Se_4W\cdot$dmf: C, 34.1; H, 2.75; N, 2.34. Found: C, 34.3; H, 2.73; N, 2.30. UV−vis (CH_2Cl_2, λ_{max}/nm, $10^{-3}\epsilon$/$M^{-1}\cdot cm^{-1}$): 310 (7.98), 468 (2.82). IR (KBr, cm^{-1}): **ν(C=O) 1665 (s),** ν(W−Se) 310 (s), 295 (m), 291 (w). ^{1}H NMR (DMSO-d_6,

(8) Hong, M. C.; Wu, M. H.; Huang, X. Y.; Jiang, F. L.; Cao, R.; Liu, H. Q.; Lu, J. X. *Inorg. Chim. Acta* **1997**, *260*, 73.
(9) (a) Hong, M. C.; Zhang, Q. F.; Cao, R.; Wu, D. X.; Chen, J. T.; Zhang, W. J.; Liu, H. Q.; Lu, J. X. *Inorg. Chem.* **1997**, *36*, 6251. (b) Zhang, Q. F.; Bao, M. T.; Hong, M. C.; Cao, R.; Song, Y. L.; Xin, X. Q. *J. Chem. Soc., Dalton Trans.* **2000**, 605.
(10) Christuk, C. C.; Ansari, M. A.; Ibers, J. A. *Angew. Chem., Int. Ed. Engl.* **1992**, *31*, 1477.
(11) Zhang, Q. F.; Leung, W. H.; Xin, X. Q.; Fun, H. K. *Inorg. Chem.* **2000**, *39*, 417.
(12) Müller, A.; Bögge, H.; Schimanski, J.; Penk, M.; Nieradzik, K.; Dartmann, D.; Krickemyer, E.; Schimanski, J.; Römer, C.; Römer, M.; Dornfeld, H.; Wienböker, U.; Hellmann, W.; Zimmermann, M. *Monatsh. Chem.* **1989**, *120*, 367.
(13) Zhang, Q. F.; Xiong, Y. N.; Lai, T. S.; Ji, W.; Xin, X. Q. *J. Phys. Chem. B* **2000**, *104*, 3476. (b) Xiong, Y. N.; Ji, W.; Zhang, Q. F.; Xin, X. Q. *J. App. Phys.* **2000**, *88*, 1225.
(14) O'Neal, S. C.; Kolis, J. W. *J. Am. Chem. Soc.* **1988**, *110*, 1971.
(15) Wang, F. T.; Najzionek, J.; Leneker, K. L.; Wasserman, H.; Braitsch, D. M. *Inorg. Synth. Met.-Org. Chem.* **1978**, *8*, 120.

Table 1. Crystallographic Data for Cluster Compounds [(μ-WSe_4)($AgPCy_3$)$_2$] (**1**), [(μ_3-WSe_4)Ag_3(PCy_3)$_3$(μ_3-I)] (**2**), [(μ_3-WSe_4)Ag_3(μ-I)(μ-dppa)$_2$]·dmf (**3**·Dmf), [(μ_3-WSe_4)Ag_3(μ_3-I)(μ-dppm)$_2$] (**4**), and [(μ_3-WSe_4)$_2Ag_4$(μ-dppm)$_3$]·dmf·CH_2Cl_2 (**5**·dmf·CH_2Cl_2)

param	**1**	**2**	**3**·dmf	**4**	**5**·dmf·CH_2Cl_2
empirical formula	$C_{36}H_{66}P_2Ag_2Se_4W$	$C_{54}H_{99}P_3IAg_3Se_4W$	$C_{51}H_{49}N_3OP_4IAg_3Se_4W$	$C_{50}H_{44}IP_4Ag_3Se_4W$	$C_{79}H_{75}NOCl_2P_6Ag_4Se_8W_2$
fw	1276.26	1791.44	1794.01	1718.93	2741.98
cryst system	triclinic	orthorhombic	monoclinic	monoclinic	monoclinic
space group	$P\bar{1}$	$Pna2_1$[c]	$P2_1/c$	$P2_1/n$	$P2_1/c$
a/Å	11.3322(12)	37.2352(5)	18.553(4)	14.4170(11)	22.732(5)
b/Å	17.1130(18)	11.7024(1)	14.078(3)	20.4544(15)	14.137(3)
c/Å	23.541(3)	14.9951(2)	21.755(4)	18.1981(13)	28.173(6)
α/deg	86.761(5)				
β/deg	77.665(6)		98.84(3)	90.708(1)	107.01(3)
γ/deg	82.528(6)				
V/Å^3	4420.2(9)	6533.98(14)	5614.6(19)	5366.0(7)	8657(3)
Z	4	4	4	4	4
μ(Mo Kα)/mm^{-1}	6.863	5.446	6.369	6.656	7.113
D_c/g·cm^{-3}	1.918	1.821	2.122	2.128	2.104
unique reflcns/R(int)	11 299/0.0544	13 601/0.0531	11 017/0.0489	9383/0.0734	18 867/0.0749
data/restraints/params	11 299/0/823	13 601/1/622	11 017/0/613	9383/0/568	18 867/0/870
R1,[a] wR2[b] [$I > 2\sigma(I)$]	0.0655, 0.1431	0.0310, 0.0513	0.0435, 0.1116	0.0470, 0.1032	0.0430, 0.0664
R1,[a] wR2[b] [all data]	0.1007, 0.1431	0.0543, 0.0569	0.0552, 0.1162	0.0736, 0.1317	0.0592, 0.0699
resid ρ/e·Å^{-3}	+3.699, −1.522	+0.645, −0.502	+2.096, −2.230	+1.413, −1.485	+1.689, −1.629

[a] $R1 = \sum^{1/2}|F_o| - |F_c|^{1/2}/\sum|F_o|$. [b] $wR2 = [\sum w(|F_o^2| - |F_c^2|)^2/\sum w|F_o^2|^2]^{1/2}$. [c] The Flack parameter of refinement structure is 0.006(4).

ppm): δ 8.05 (s, 1H, C*H*O), 8.01 (br, 2H, N*H*), 7.33−7.51 (m, 40H, Ph), 2.99 (s, 6H, *Me*$_2$NCHO). ^{31}P NMR (DMSO-d_6, ppm): δ 44.9, 48.2. ^{77}Se NMR (DMSO-d_6, ppm): δ 1692, 1008, 829. MS (FAB): m/z 1722 ($M^+ + 1$).

Synthesis of [(μ_3-WSe_4)Ag_3(μ_3-I)(μ-dppm)$_2$] (4). The method was similar to that used for **3**, employing dppm (118 mg, 0.30 mmol) instead of dppa. Yield: 135 mg (39%). Anal. Calcd for $C_{50}H_{44}P_4IAg_3Se_4W$: C, 34.9; H, 2.56. Found: C, 35.1; H, 2.63. UV−vis (DMF, λ_{max}/nm, $10^{-3}\epsilon/M^{-1}\cdot cm^{-1}$): 318 (6.59), 456 (2.65). IR (KBr, cm^{-1}): ν(C=**O) 1667 (s),** ν(W−Se) 308 (s), 297 (m), 292 (w). ^{1}H NMR (DMSO-d_6, ppm): 7.30−7.52 (m, 40H, Ph), 5.43 (s, 4H, C*H*$_2$). ^{31}P NMR (DMSO-d_6, ppm): δ 3.33, 6.45. ^{77}Se NMR (DMSO-d_6, ppm): δ 1699, 1013, 825. MS (FAB): m/z 1718 ($M^+ + 1$).

Synthesis of [(μ_3-WSe_4)$_2Ag_4$(μ-dppm)$_3$]·dmf·CH_2Cl_2 (5·dmf·CH_2Cl_2). To a solution of $[Et_4N]_2[WSe_4]$ (150 mg, 0.20 mmol) in DMF (10 mL) was added a mixture of $AgNO_3$ (68 mg, 0.40 mmol) and dppm (160 mg, 0.40 mmol) in CH_2Cl_2 (15 mL). After the reaction had been stirred for 10 min at room temperature, it was filtered through a filter paper to provide a red filtrate. Slow addition of a mixture solvent of THF/Et_2O (1:5) afforded dark red needle crystals suitable for a single-crystal X-ray diffraction analysis, which were identified as **5**·dmf·CH_2Cl_2. Yield: 152 mg (90%). Anal. Calcd for $C_{75}H_{66}P_6Ag_6Se_8W_2$·dmf·$CH_2Cl_2$: C, 34.6; H, 2.76; N, 0.51. Found: C, 34.2; H, 2.74; N, 0.50. UV−vis (CH_2Cl_2, λ_{max}/nm, $10^{-3}\epsilon/M^{-1}\cdot cm^{-1}$): 321 (6.72), 457 (2.85). IR (KBr, cm^{-1}): ν(C=**O) 1668 (s),** ν(W−Se) 312 (s), 296 (m), 293 (w). ^{1}H NMR (DMSO-d_6, ppm): δ 8.07 (s, 1H, C*H*O), 7.27−7.55 (m, 84H, Ph), 5.32 (s, 2H, C*H*$_2$Cl$_2$), 5.45 (s, 6H, C*H*$_2$), 3.05 (s, 6H, *Me*$_2$NCHO). ^{31}P NMR (DMSO-d_6, ppm): δ 7.12, 8.97, 12.9. ^{77}Se NMR (DMSO-d_6, ppm): δ 1677, 1016, 951. MS (FAB): m/z 2585 ($M^+ + 1$).

Structure Determinations. The structures of **1**, **2**, **3**·dmf, **4**, and **5**·dmf·CH_2Cl_2 were obtained by the single-crystal X-ray diffraction technique. Crystals were mounted on the tips of glass fibers. Data for **1**, **2**, and **4** were collected at 293 K on a Bruker SMART-CCD area-detector diffractometer with a graphite monochromator using Mo Kα radiation (λ = 0.710 73 Å). Data for **3**·dmf and **5**·dmf·CH_2Cl_2 were collected on a Siemens Stoe-IPDS diffractometer (Mo Kα radiation, λ = 0.710 73 Å) equipped with an imaging plate area detector and a rotating anode. All structures were solved by the use of direct methods; refinement was performed by the full-matrix least-squares methods on F^2 with the SHELXTL software package.[16] All non-hydrogen atoms were refined anisotropically. The positions of all hydrogen atoms were generated geometrically (C_{sp^3}-H = 0.96, C_{sp^2}-H = 0.93, and N−H = 0.86 Å) and included in the structure factor calculations with assigned isotropic thermal parameters but were not refined. The largest peaks in the final difference maps had heights of 3.699 (for **1**), 2.096 (for **3**·dmf), and 1.689 e Å^{-3} (for **5**·dmf·CH_2Cl_2) and are in the vicinity of the W atoms. Crystallographic data are summarized in Table 1.

Optical Measurements. A CH_2Cl_2 solution of the cluster **4** or **5** was placed in a 5 mm quartz cuvette for optical limiting property measurements which were performed with linearity polarized 7 ns pulses at 532 nm generated from a Q-switched frequency-doubled Nd:YAG laser. The cluster is stable toward air and laser light under experimental conditions. The spatial profiles of the pulsed laser were focused on the sample cell with a 15 cm focal length mirror. The spot radius of the laser beam was measured to be 55 μm (half-width at 1/e^2 maximum). The energies of the input and output pulses were measured simultaneously by precision laser detectors (Rjp-735 energy probes) while the incident energy was varied by a Newport Com. attenuator.[17] The interval between the laser pulses was chosen to 10 s to avoid influence of thermal and long-term effects.

The effective third-order NLO absorptive and refractive properties of clusters were recorded by moving the sample along the axis of the incident laser beam (z direction), with respect to the focal point instead of being positioned at its focal point, and an identical setup was adopted in the experiments to measure the z-scan data. An aperture of 0.5 mm radius was placed in front of the detector to assist the measurement of the nonlinear optical absorption and self-focusing effect. The samples were also tested in the pump−probe experiment in which a Q-switched, mode-locked, frequency-doubled Nd:YAG laser was used to produce 532 nm pulses of 35 ps duration.[18] A standard pump−probe arrangement was employed,

(16) Sheldrick, G. M. *SHELXTL-97, Software Reference Manual*, version 5.1; Bruker AXS, Inc.: Madison, WI, 1997.
(17) (a) Sheik-Bahae, M.; Said, A. A.; Van Stryland, E. W. *Opt. Lett*. **1989**, *14*, 955. (b) Sheik-Bahae, M.; Said, A. A.; Wei, T. H.; Hagan, D. J.; Van Stryland, E. W. *IEEE J. Quantum Electron*. **1990**, *26*, 760.
(18) (a) Hou, H. W.; Liang, B.; Xin, X. Q.; Yu, K. B.; Ge, P.; Ji, W.; Shi, S. *J. Chem. Soc., Faraday Trans.* **1996**, *92*, 2343. (b) Xia, T.; Dogariu, A.; Mansour, K.; Hagan, D. J.; Said, A. A.; Van Stryland, E. W.; Shi, S. *J. Opt. Soc. Am. B* **1998**, *15*, 1497. (c) Ji, W.; Du, H. J.; Tang, S. H.; Shi, S. *J. Opt. Soc. Am. B* **1995**, *12*, 876.

Scheme 1. Reagents and Conditions[a]

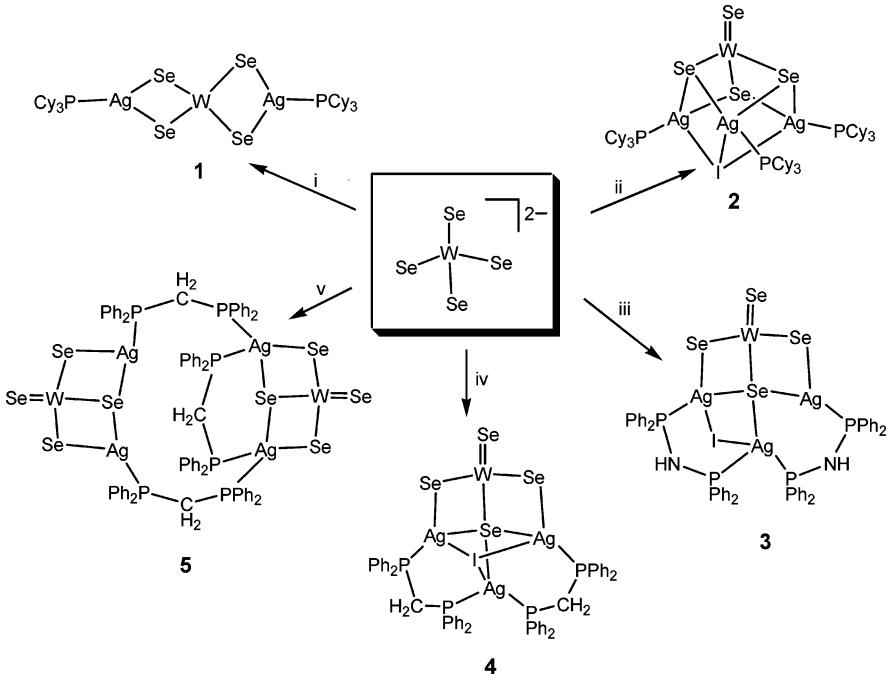

[a] Key: (i) $AgNO_3$, PCy_3/CH_2Cl_2; (ii) $AgNO_3$, PCy_3, $[Et_4N]I/CH_2Cl_2$; (iii) AgI, dppa/DMF, CH_2Cl_2; (iv) AgI, dppm/DMF, CH_2Cl_2; (v) $AgNO_3$, dppm/DMF, CH_2Cl_2.

where the peak irradiance of the probe pulse is approximately 5% of that of the pump pulse. The transmission detector was placed at 35 cm from the focus, and no aperture was mounted in the experiments.

Results and Discussion

Synthesis. Scheme 1 illustrates synthetic reactions of tetraselenotungstate anion with silver(I) species in the presence of phosphine ligands. Linear trinuclear heteroselenometallic compounds can be classified into three types, two tetrahedral metals, one tetrahedral metal and one trigonal metal, and two trigonal metals mutually *trans*-bonded the $[MSe_4]^{2-}$ anion moiety, respectively, according to the coordination geometry of the coinage-metal ions.[2c] Reaction of $[MSe_4]^{2-}$ with Cu^+ or Ag^+ in the presence of excess monodentate phosphine ligands results in the formation of $[(\mu\text{-}MSe_4)(M'PR_3)\{Ag(PR_3)_2\}]$[4] and $[(\mu\text{-}MSe_4)\{M'(PR_3)_2\}]$.[3] However, $[(\mu\text{-}MSe_4)(M'PR_3)_2]$[4a,12] (M = Mo, W; M′ = Cu, Ag; R_3 = Ph_3, $PhMe_2$) that contain two trigonally coordinated coinage metals are obtained by a similar reaction with the coinage-metal to phosphine ligand ratio strictly 1:1. Treatment of $[WSe_4]^{2-}$ with a mixture of $AgNO_3$ and PCy_3 in a 1:1 ratio in the absence of halide afforded a linear trinuclear compound $[(\mu\text{-}WSe_4)(AgPCy_3)_2]$ (**1**). A similar reaction in the presence of iodide ion gave rise to the isolation of the cubanelike cluster $[(\mu_3\text{-}WSe_4)Ag_3(PCy_3)_3(\mu_3\text{-}I)]$ (**2**), regardless of the molar ratio of $[WSe_4]^{2-}$ to $AgNO_3/PCy_3$ originally taken, within the range of 1:1 to 1:4. In **2**, the μ_3-iodide coordinated to the silver atoms occupies one vertex of the cubane core and balances the overall charge of the cluster, suggesting that the cubanelike structure is quite stable.[3a,6,7]

Attempts to synthesize polynuclear cage cluster compounds by reacting $[Et_4N]_2[WSe_4]$ with the in situ generated $Ag(I)-PCy_3$ species in the absence or presence of halide were unsuccessful. Treatment of $[Et_4N]_2[WSe_4]$ with AgI in the presence of the bidentate phosphine ligand dppa afforded a neutral tetranuclear compound $[(\mu_3\text{-}WSe_4)Ag_3(\mu\text{-}I)(\mu\text{-dppa})_2]$ (**3**). A similar reaction using dppm ligand gave an analogous tetranuclear compound $[(\mu_3\text{-}WSe_4)Ag_3(\mu_3\text{-}I)(\mu\text{-dppm})_2]$ (**4**). As reported previously, a mixture of AgI and bidentate phosphine ligands L (e.g. L = dppa or dppm) in solutions was found to contain predominately the trinuclear species $[Ag_3(\mu_3\text{-}I)_2(\mu\text{-}L)_3]^+$.[19] Therefore, we believe that the formation of **3** and **4** involved the metathetical reaction of $[Ag_3(\mu_3\text{-}I)_2(\mu\text{-}L)_3]^+$ with the $[WSe_4]^{2-}$ anion. It seems that the displacement of one iodide and one L in $[Ag_3(\mu_3\text{-}I)_2(\mu\text{-}L)_3]^+$ gave an unsaturated intermediate $[Ag_3(\mu_3\text{-}I)(\mu\text{-dppx})_2]^{2+}$ that subsequently coordinated to $[WSe_4]^{2-}$. Further support for this speculation comes from the X−ray crystallographic analyses of compounds **3** and **4**, which revealed that the trigonal Ag_3 core in these compounds was maintained after the cluster formation (vide infra). Similarly, reaction of $[Et_4N]_2[WSe_4]$ with the in situ generated Ag(I)−dppm species in the absence of iodide source afforded a neutral hexanuclear compound $[(\mu_3\text{-}WSe_4)_2Ag_4(\mu\text{-dppm})_3]$ (**5**) in a good yield (90%). It is noted that Lang reported the formation of two different W/Ag/S compounds by the same reaction under different conditions.[20] Hexanuclear heterothiometallic cluster $[(WS_4)_2Ag_4(dppm)_3]$ was isolated in a low yield from low-heating-temperature solid-state reaction of $(NH_4)_2[WS_4]$, $[Ag(MeCN)_4](PF_6)$, and dppm (in a ratio of 1:2:4). However,

(19) (a) Franzoni, D.; Pelizi, G.; Predieri, G.; Tarasconi, P.; Vitali, F.; Pelizzi, C. *J. Chem. Soc., Dalton Trans.* **1989**, 247. (b) Zhou, W. B.; Dong, Z. C.; Song, J. L.; Zeng, H. Y.; Cao, R.; Guo, G. C.; Huang, J. S.; Li, J. *J. Cluster Sci*. **2002**, *13*, 119.

(20) Yu, H.; Xu, Q. F.; Sun, Z. R.; Ji, S. J.; Chen, J. X.; Liu, Q.; Lang, J. P.; Tatsumi, K. *Chem. Commun*. **2001**, 2614.

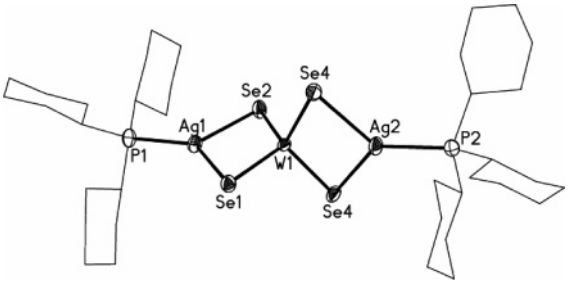

Figure 1. Molecular structure of $[(\mu\text{-}WSe_4)(AgPCy_3)_2]$ (**1**).

the same reaction carried out in DMF/CH_2Cl_2 solution gave a tetranuclear cluster $[(WS_4)Ag_4(dppm)_4](PF_6)$ in which two dppm ligands bind to two silver atoms in a κ^1 fahsion.[20] In the present system, dppm seems to act as a bridging ligand for the construction of a binuclear $[Ag_2L]^{2+}$ species obtained from the 1:1 mixture of $AgNO_3$ and dppm. Subsequently, self-assembly of this binuclear Ag(I) species with $[WSe_4]^{2-}$ anion gave the hexanuclear compound **5**. The use of a deficiency of dppm ligand or longer reaction time led to a lower yield of compound **5** along with uncharacterized black precipitate, indicating that the selenide is relatively more reactive than the sulfide analogue in the silver−dppm system. Compounds **1**−**5** are very air stable in both the solid state and solution. The differences in reactivity and stability between the W/Se/Ag and W/S/Ag systems may result from the larger size of the selenium atom versus that of sulfur atom.[2,3]

Crystal Structures. The structure of $[(\mu\text{-}WSe_4)(AgPCy_3)_2]$ (**1**) is shown in Figure 1. Similar structure has been found in analogous heterometallic $[MQ_4]^{2-}$ (Q = S, Se) compounds,[3,4,21] e.g. $[(\mu\text{-}WSe_4)(AgPPh_3)_2]$[12] and $[(\mu\text{-}WSe_4)(AgPPh_3)\{Ag(PPh_3)_2\}]$.[4b] Compound **1** crystallizes in the triclinic crystal system. There are two perpendicular arrangements of the molecules in the crystal with slightly different conformations. No significant differences in bonding parameters between these two molecules (A and B) were found. **1** comprises two $Ag(PCy_3)$ fragments ligating the opposite edges of a tetrahedral $[WSe_4]^{2-}$ moiety. Distances from W center atom to the four bridging Se atoms range from 2.317(3) to 2.353(3) Å, while the Se−W−Se angles range from 106.95(11) to 114.04(10)°. The geometry about Ag atoms may be described as distorted trigonal planar with small Se−Ag−Se angles [99.33(9) and 99.96(10)° for molecule A and 98.55(10) and 99.74(10)° for molecule B]. The three metal atoms and two phosphorus atoms are approximately collinear with the Ag···W···Ag angle of 177.71(6)° and the P−Ag···W angles of 170.23(17) and 175.58(17)° in molecule A. The W···Ag distances are 2.918(2) and 2.925(2) Å for molecule A and 2.935(2) and 2.936(2) Å for molecule B, which are comparable to those of the related clusters comprising trigonal coordination silver atoms.[4b,12,21]

The structure of $[(\mu_3\text{-}WSe_4)Ag_3(PCy_3)_3(\mu_3\text{-}I)]$ (**2**) is shown in Figure 2. The neutral cluster molecule contains a highly distorted cubanelike $[WAg_3Se_3I]^{2-}$ core with a terminal

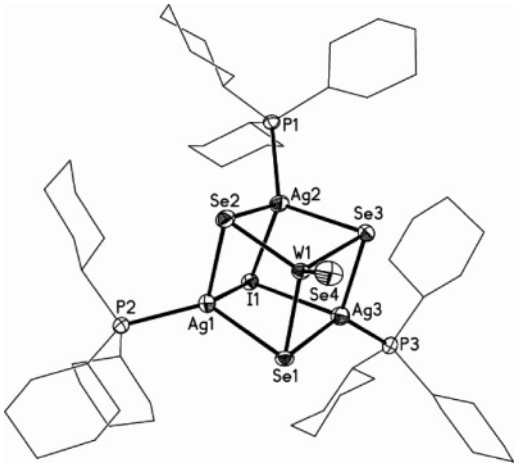

Figure 2. Molecular structure of $[(\mu_3\text{-}WSe_4)Ag_3(PCy_3)_3(\mu_3\text{-}I)]$ (**2**).

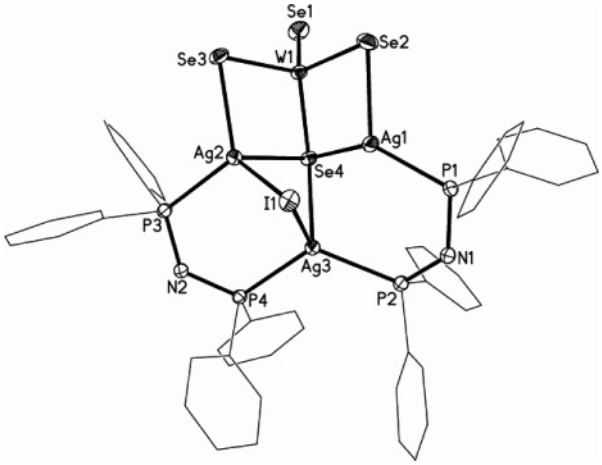

Figure 3. Molecular structure of $[(\mu_3\text{-}WSe_4)Ag_3(\mu\text{-}I)(\mu\text{-}dppa)_2]$ (**3**).

W═Se group and a PCy_3 ligand bound to each Ag atom. Examples of related cubanes containing $[MSe_4]^{2-}$ (M = Mo, W) moieties are known.[3a,6,7] In the $[WAg_3Se_3I]$ core, both the Ag and W atoms are tetrahedrally coordinated. The average W−μ_3-Se distance of 2.3691(7) Å is obviously longer than the W−Se_t (terminal) distances of 2.252(1) Å. The average W···Ag distances in **2** (3.026(1) Å) is comparable to those in other cubanelike argentoselenotungates such as $[(\mu_3\text{-}WSe_4)Ag_3(PPh_3)_3(\mu_3\text{-}Cl)]$[7e] (3.010(3) Å) and $[(\mu_3\text{-}WSe_4)Ag_3(PPhMe_2)_3(\mu_3\text{-}I)]$[6a] (2.976(1) Å). The high distortion of the cubane compound **2**, as a character of structural stability, results in three unequalaterally long Ag−I distances [2.987(1), 3.156(1), and 3.240(1) Å] along with three small vertex angles about the I atom [71.23(1), 68.12(2), and 67.54(1)°].

The structures of **3**·dmf and **4** have been confirmed by an X-ray diffraction study. The molecular structures of **3** and **4** are shown in Figures 3 and 4, respectively. The structural frames in both neutral compounds **3** and **4** have an open butterfly configuration. The structure of **3** consists of a metal-trigonal $[Ag_3(\mu\text{-}I)(\mu\text{-}dppa)_2]^{2+}$ fragment ligating a tetrahedral $[WSe_4]^{2-}$ moiety whereas that of **4** contains a metal-trigonal $[Ag_3(\mu_3\text{-}I)(\mu\text{-}dppm)_2]^{2+}$ moiety. The coordination geometry of the W atom in **3** or **4** remains nearly tetrahedral within error and is more distorted than those in other argentoselenometallic clusters,[9−12] indicated by ca. 8° deviation among

(21) (a) Müller, A.; Schimanski, U.; Schimanski, J. *Inorg. Chim. Acta* **1983**, *76*, L245. (b) Müller, A.; Wienböker, U.; Penk, M. *Chimia* **1989**, *43*, 50.

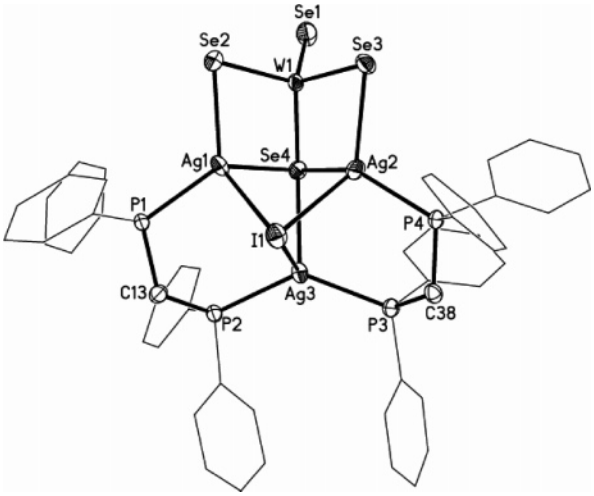

Figure 4. Molecular structure of $[(\mu_3\text{-}WSe_4)Ag_3(\mu_3\text{-}I)(\mu\text{-}dppm)_2]$ (**4**).

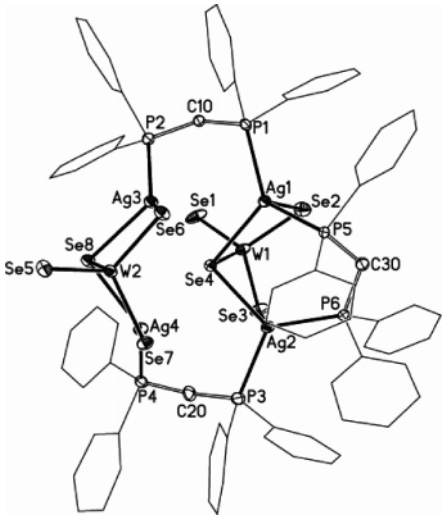

Figure 5. Molecular structure of $[(\mu_3\text{-}WSe_4)_2Ag_4(\mu\text{-}dppm)_3]$ (**5**).

Se−W−Se angles ranging from 104.77(3) to 112.72(3)° in **3** and from 104.69(6) to 112.75(4)° in **4**. The W−Se bond lengths fall into three categories: the W−Se_t, W−μ-Se, and W−μ_4-Se bond distances are 2.265(1), 2.336(1) (average), and 2.401(1) Å, respectively, in **3** and the according parameters are 2.260(1), 2.334(1) (average), and 2.416(1) Å, respectively, in **4**. There are three different types of silver atoms in **3**: one has trigonal planar geometry, being bonded to two selenium atoms and one phosphorus atom, whereas the other two have tetrahedral geometry, of which one is bonded to two selenium atoms, one phosphorus atom, and one iodine atom and the other is bonded to one selenium atom, two phosphorus atoms, and one iodine atom. In **4**, three silver atoms are highly distorted tetrahedral with angles around silvers ranging from 90.79(7) to 130.52(10)°. The Ag−Se distances in **3** are clearly influenced by the coordination modes of the Se and Ag: the Ag−Se distances involving μ-Se and 3-coordinate Ag, μ-Se and 4-coordinate Ag, μ_4-Se and 3-coordinate Ag, and μ_4-Se and 4-coordinate Ag are 2.585(1), 2.618(1), 2.652(1), and 2.722(1) Å, respectively. The Ag(3)−μ_4-Se(4) of 2.896(1) Å in **3** is comparable to those observed in related systems, such as $Ag_{11}(\mu_5\text{-}Se)(Et_2CNS_2)_9$ [Ag-μ_5-Se: 2.656(4)−2.898(4) Å][22] and $Ag_8(\mu_8\text{-}Se)[Se_2P(O^iPr)_2]_6$ [Ag-μ_8-Se: 2.624(1)−2.868(1) Å].[23] The Ag(3)−μ_4-Se(4) of 2.969(2) Å in **4** is slightly longer than that in **3**. In **3**, the W···Ag separation for the 3-coordinate silver of 2.9609(9) Å is slightly shorter than that for the 4-coordinate counterpart (3.023(1) Å). The W···Ag separation (2.972(1) Å) for the 4-coordinate silver in **4** is comparable to those containing 4-coordinate silvers in $[(\mu_3\text{-}WSe_4)(AgPPhMe_2)_3(\mu_3\text{-}I)]$ (2.976(1) Å)[6a] and $[(\mu_3\text{-}WSe_4)(AgPPh_3)_3(\mu_3\text{-}Br)]$ (2.984(3) Å).[7c] It is significant to note that the Ag···Ag separations [Ag(1)···Ag(3) = 3.070(1) and Ag(2)···Ag(3) = 3.075(1) Å in **3**, Ag(1)···Ag(3) = 3.377(1) and Ag(2)···Ag(3) = 3.052(1) Å in **4**] are comparable to those in $[Ag_3(dppm)_3(\mu_3\text{-}\eta^1\text{-}C{\equiv}C{-}R)_2]^{2+}$ [average 3.048(1) Å][24] and in $[Ag_3(\mu_3\text{-}I)_2(dppm)_3]^+$ [average 3.236(1) Å].[19b]

The iodine atom bridges two silver atoms with an acute Ag−I−Ag bond angle of 64.10(2)°, and the average Ag−μ-I distance of 2.915(1) Å in **3** is shorter than the average Ag−μ_3-I distance of 3.128(1) Å in **2**. The average Ag−μ_3-I distance and Ag−μ_3-I−Ag angle in **4** are 3.096(1) Å and 63.86(3)°, respectively.

The solid-state structure of **5**·dmf·CH_2Cl_2 has been established by X-ray crystallography. The molecular structure consists of a neutral cluster and lattice solvents. Although a similar structure has been previously found in $[(WS_4)_2Ag_4(dppm)_3]$,[20] the current arrangement appears to the first example of polynuclear argentoselenometallic clusters with the $[MSe_4]^{2-}$ moieties. The structure of $[(\mu_3\text{-}WSe_4)_2Ag_4(\mu\text{-}dppm)_3]$ (**5**) is illustrated in Figure 5. The structure of **5** comprises two WSe_4Ag_2 cluster fragments and three dppm ligands. Two dppm ligands link to the two interconnected silver atoms between the two WSe_4Ag_2 moieties while the other one links to two silver atoms within a WSe_4Ag_2 moiety. Each $[WSe_4]^{2-}$ unit acts as a tridentate ligand binding to two silver atoms, leaving a terminal W═Se bond. The coordination geometry of the W centers remains nearly tetrahedral, with the Se−W−Se angles ranging from 106.95(5) to 113.11(4)°. The average W−Se_t, W−μ-Se, and W−μ_3-Se bond distances are 2.268(1), 2.333(1), and 2.399(1) Å, respectively. There are two types of coordination geometry for Ag: distorted tetrahedral and approximate trigonal planar. The average Ag−Se distance of 2.727(1) Å involving tetrahedral silver atoms is obviously longer than that of 2.614(2) Å involving trigonal planar silver atoms. Accordingly, the W···Ag distance for the 4-coordinate Ag (average 3.120(1) Å) is slightly longer than that for the 3-coordinate counterpart (average 2.994(1) Å), as found in **3** and a variety of related clusters.[5,11,12] The Ag−P distances in **5** are slightly influenced by the silver coordination modes. The average Ag−P distance of 2.414(3) Å for 3-coordinate Ag is shorter than that of 2.478(3) Å for the 4-coordinate counterpart. The distance of 3.514 Å between the nearest two silver atoms is

(22) Zhang, Q. F.; Cao, R.; Hong, M. C.; Su, W. P.; Liu, H. Q. *Inorg. Chim. Acta* **1998**, *277*, 171.
(23) Liu, C. W.; Shang, I. J.; Wang, J. C.; Keng, T. C. *Chem. Commun.* **1999**, 995.
(24) Yam, V. W. W.; Fung, W. K. M.; Cheung, K. K. *Organometallics* **1997**, *16*, 2032.

Table 2. Comparison of Selected Bond Parameters for Compounds **1**−**5**[a]

compd	W−Se$_t$[b]	W−Se$_b$[b]	Ag−Se	Ag−P	W···Ag	Se−W−Se	Se−Ag−Se
1		2.317(3)−2.353(3) av 2.327(3)	2.516(3)−2.586(3) av 2.551(3)	2.376(6)−2.393(6) av 2.385(6)	2.918(2)−2.936(2) av 2.928(2)	106.38(11)−114.04(10) av 109.49(10)	98.55(10)−99.96(10) av 99.40(10)
2	2.252(1)	2.354(1)−2.391(1) av 2.369(1)	2.601(1)−2.739(1) av 2.652(1)	2.400(2)−2.428(1) av 2.410(2)	2.980(1)−3.114(1) av 3.026(1)	107.05(2)−112.74(2) av 109.43(2)	89.54(2)−98.51(2) av 95.34(2)
3·dmf	2.265(1)	2.328(1)−2.401(1) av 2.361(1)	2.595(1)−2.896(1) av 2.670(1)	2.400(2)−2.472(2) av 2.440(2)	2.961(1)−3.023(1) av 2.992(1)	104.77(3)−1 12.72(3) av 109.43(3)	95.19(3)−97.25(3) av 96.22(3)
4	2.260(1)	2.331(1)−2.416(1) av 2.358(1)	2.615(2)−2.656(1) av 2.636(2)	2.405(3)−2.498(3) av 2.448(3)	2.970(1)−2.973(1) av 2.972(1)	104.69(6)−112.75(4) av. 109.45(5)	97.09(5)−97.24(5) av 97.16(5)
5·dmf·CH_2Cl_2	2.260(1)−2.276(1) av 2.268(1)	2.315(1)−2.403(1) av 2.355(1)	2.583(1)−2.787(1) av 2.671(1)	2.414(3)−2.482(3) av 2.455(3)	2.984(1)−3.154(1) av 3.057(1)	106.95(5)−113.11(4) av 109.44(5)	85.27(4)−106.88(4) av 94.70(4)

[a] Bond distances in Å and bond angles in deg with esd's in parentheses. [b] t = terminal; b = bridging.

too long for a direct Ag−Ag bond. Selected bond distances and angles for compounds **1**−**5** are complied in Table 2 for comparison.

Spectroscopic Properties. The metal−selenium stretching modes of the selenometallic compounds can be identified since they appear as strong and sharp absorptions in the low-wavenumber region below 400 cm^{-1}.[3,9,25] The W−Se stretching vibrations for **1**−**5** were expectedly found in the region of 290−315 cm^{-1} of their infrared spectra. The terminal W−Se$_t$ absorptions at 313 cm^{-1} for **2**, 310 cm^{-1} for **3**, 308 cm^{-1} for **4**, and 312 cm^{-1} for **5** appear at relatively high wavenumbers compared to the ν(W−Se) absorption at 305 cm^{-1} in the $[WSe_4]^{2-}$ anion.[1a] The bridging W−μ_n-Se (n = 2−4) vibrations are observed in the range 290−300 cm^{-1}, which are lower than that for free $[WSe_4]^{2-}$.[1a] The infrared spectra of in **3**·dmf and **5**·dmf·CH_2Cl_2 display typical absorption peaks at about 1666 cm^{-1}, which are characteristic for ν(C═O) stretching vibration of cocrystallization DMF solvents.

The electronic spectra of compounds **1**−**5** in CH_2Cl_2 solution show intense absorption bands at 250−500 nm, as shown in Figure 6. The very intense peaks at 310−320 nm may be assigned to the Se → W charge-transfer arising from the $[WSe_4]^{2-}$ moiety in the cluster compounds, whereas the weaker broad bands at 450−470 nm may be ascribed to a relatively weak $[WSe_4]^{2-}$ to silver interaction. Similar spectral assignments have been made for related argentoselenotungstate clusters.[3a,4−6] It is interesting to note that the

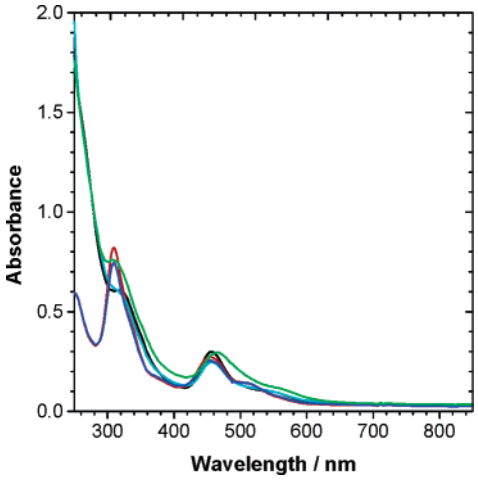

Figure 6. Electronic absorption (UV−vis) spectra of **1** (blue), **2** (red), **3** (green), **4** (cyan), and **5** (black), all at 1.0 × 10^{-3} M in CH_2Cl_2. The optical path is 1 cm.

$[WSe_4]^{2-}$ → Ag charge-transfer transition peaks in the present clusters are obviously blue-shifted by the comparison of the $[WS_4]^{2-}$ → Ag charge-transfer transition peaks (350−360 nm) in the sulfur analogues,[1c] while peaks at 450−470 nm were found to be slightly red-shifted when silver atoms in the argentoselenotungstate clusters are replaced by copper atoms in the cuproselenotungstate clusters (485−495 nm).[3a,7d]

The ^{1}H NMR spectra for clusters **1**−**5** are very similar to those of the free ligands, PCy_3, dppa, and dppm, indicating that all clusters are diamagnetic and that the geometric structures of the clusters cores have little influence on the proton chemical shielding of coordination ligands. The ^{31}P{^{1}H} NMR spectrum of **1** shows one singlet at 55.4 ppm, suggesting that there are two magnetically equivalent phosphorus atoms in this linear trinuclear cluster. The cubanelike cluster **2** displays a single peaks at 44.8 ppm in its ^{31}P{^{1}H} NMR spectrum, consistent with its solid-state structure. Two ^{31}P signals at 48.2 and 44.9 ppm for **3** are assigned to the four- and three-coordination phosphorus atoms, respectively. Similarly, two single peaks at 3.33 and 6.45 ppm in the ^{31}P NMR spectrum of **4** may be ascribed to the two phosphorus atoms with different coordination environments. Three board peaks at 7.12, 8.97, and 12.91 ppm were observed in the ^{31}P NMR spectrum of **5**, indicating that there three types of coordination environments for the phosphorus atoms. On the basis of the present survey, it can be inferred that the ^{31}P chemical shifts for argentoselenometallic phosphine compounds are sensitive to coordination environment of the silver atoms.[4]

The ^{77}Se NMR spectrum of cluster **1** has a singlet peak at 1135 ppm which is compatible to that at 1092 ppm in [(μ-WSe_4)($AgPPhMe_2$)$_2$] with a similar structure.[3a,c] As expected, two peaks at 1664 and 1058 ppm were found in the ^{77}Se NMR spectrum of **2**, which are assigned to the terminal Se and μ_3-Se nuclei, respectively, because the bridging Se atoms are shielded and the terminal Se atoms are deshielded relative to the Se nuclei in the symmetric anion $[WSe_4]^{2-}$ (δ = 1235 ppm).[26] Similarly, the ^{77}Se NMR spectra of **3** and **4** show three peaks at 1692, 1008, and 829 ppm for **3** and at 1699, 1013, and 825 ppm for **4** which may be ascribed to the terminal Se, μ-Se, and μ_4-Se atoms, respectively. The ^{77}Se NMR spectrum of **5** shows three peaks at 1677, 1016, and 951 ppm which may be attributable to the terminal Se, μ-Se,

(25) Ansari, M. A.; Chau, C.-N.; Mahler, C. H.; Ibers, J. A. *Inorg. Chem.* **1989**, *28*, 650.
(26) Ansari, M. A.; Mahler, C. H.; Chorghade, G. S.; Lu, Y.-J.; Ibers, J. A. *Inorg. Chem.* **1990**, *29*, 3832.

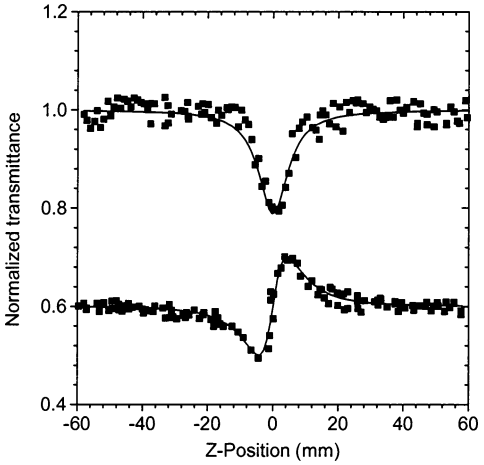

Figure 7. *z*-scan data for 6.5×10^{-4} M of **4** in CH_2Cl_2 at 532 nm with I_0 being 1.4×10^{12} W/m^2, the top collected under the open aperture configuration showing NLO absorption and the bottom obtained by dividing the normalized *z*-scan data obtained under the closed aperture configuration by the normalized *z*-scan data in the top. The solid curves are theoretical fits based on *z*-scan theoretical calculations.

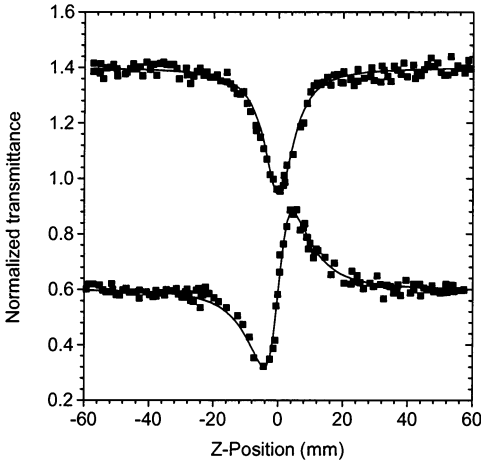

Figure 8. *z*-scan data for 6.5×10^{-4} M of **5** in CH_2Cl_2 at 532 nm with I_0 being 1.4×10^{12} W/m^2, the top collected under the open aperture configuration showing NLO absorption and the bottom obtained by dividing the normalized *z*-scan data obtained under the closed aperture configuration by the normalized *z*-scan data in the top. The solid curves are theoretical fits based on *z*-scan theoretical calculations.

and μ_3-Se nucleus, respectively. The FAB^+ mass spectra of compounds **1**−**5** exhibit molecular ions corresponding to $M^+ + 1$ with the characteristic isotopic distribution patterns.

NLO Properties. The NLO properties of compounds **4** and **5** with new structural types were investigated by using the *z*-scan technique.[17,18] The nonlinear absorption component was evaluated under an open aperture configuration. Theoretical curves of transmittance against the *z*-position, eqs 1 and 2, were fitted to the observed *z*-scan data by varying the effective third-order NLO absorptivity α_2 value, where the experimentally measured α_0 (linear absorptivity), L (the optical path of sample), and $I_i(Z)$ (the on-axis irradiance at z-position) were adopted:

$$T(Z) = (1/\pi^{1/2}q(Z)) \int_{-\infty}^{\infty} \ln[1 + q(Z)]e^{-\tau^2}\, d\tau \qquad (1)$$

$$q(Z) = \alpha_2 I_0 \frac{(1 - e^{-\alpha_0 L})}{\alpha_0} \qquad (2)$$

The solid line in Figure 7 (up) is the theoretical curve calculated with $\alpha_2 = 6.2 \times 10^{-4}$ cm W^{-1} for the concentrations 6.5×10^{-4} M for **4** in CH_2Cl_2 solution. The nonlinear refractive component of **4** was assessed by dividing the normalized *z*-scan data obtained in the close-aperture configuration by those obtained in the open-aperture configuration. The nonlinear refractive component plotted with the filled squares in Figure 7 (down) was assessed by dividing the normalized *z*-scan data obtained under the closed aperture configuration by the normalized *z*-scan data obtained under the open aperture configuration. The valley and peak occur at about equal distances from the focus. It can be seen that the difference in valley−peak positions ΔZ_{V-P} is 9.3 mm (see Figure 7), fitting eq 3,

$$\Delta Z_{V-P} = 1.72 \frac{\pi \omega_0^{\,2}}{\lambda} \qquad (3)$$

where ω_0 is the laser beam waist radius (35 ± 5 μm) and the laser wavelength (532 nm). This result suggests that observed optical nonlinearity has a third-order dependence on the incident electric field.[17b] The difference between normalized transmittance values at valley and peak positions $\Delta T_{V-P} = 0.20$ for **4**, which is related to nonlinear refractive index n_2 (cm^2 W^{-1}) by eqs 4 and 5,

$$\Delta T_{V-P} = 0.406|\Delta\Phi_0| \qquad (4)$$

$$\Delta\Phi_0 = \frac{2\pi}{\lambda} I_0 \frac{1 - e^{-\alpha_0 L}}{\alpha_0} n_2 \qquad (5)$$

where $\Delta\Phi_0$ and I_0 (1.2×10^8 W cm^{-1}) are the on-axis phase shift and on-axis irradiance, both on focus, respectively, and α_0 (0.3 cm) and L (0.1 cm) are the linear absorption coefficient and optical path of the sample.[17b] Accordingly, the solid curve is an eye guide for comparison where the effective nonlinear refractivity n_2 value estimated therefore is 6.7×10^{-10} cm^2 W^{-1} for **4**. Experiments with varied I_0 show that n_2 so measured is indeed independent of I_0, consistent with the notion that $n = n_0 + n_2 I$ and the observed NLO phenomenon is third order in nature. These results suggest an effectively modest third-order optical nonlinearity. Similarly, the solid line in Figure 8 (up) is the theoretical curve calculated with $\alpha_2 = 8.9 \times 10^{-4}$ cm W^{-1} for the concentrations 6.5×10^{-4} M for **5** in CH_2Cl_2 solution. The nonlinear refractive component plotted with the filled squares in Figure 8 (down) was assessed by dividing the normalized *z*-scan data obtained under the closed aperture configuration by the normalized *z*-scan data obtained under the open aperture configuration. It can be also seen that the difference in valley−peak positions ΔZ_{V-P} is 9.0 mm and the difference between normalized transmittance values at valley and peak positions $\Delta T_{V-P} = 0.55$ for **5**. The solid curve is an eye guide for comparison where the effective nonlinear refractivity n_2 value estimated therefore is 1.8×10^{-9} cm^2 W^{-1} for **5**. By comparison of the NLO results of **4**, the results of hexanuclear cluster **5** suggest an effectively strong third-order

Table 3. Comparison of Nonlinear Optical Parameters for **1**, **2**, **4**, **5**, and Related Argentoseleno(thio)metallic Cluster Compounds[a]

cluster compd	structural type	α_2/cm W^{-1}	n_2/cm^2 W^{-1}	linear transm/%	limiting threshold/J cm^{-2}	ref
[(μ-WSe_4)($AgPPh_3$){$Ag(PPh_3)_2$}]	linear	7.8×10^{-5}	8.7×10^{-10}	60	1.4	4b
[(μ-WSe_4)($AgPCy_3$)$_2$] (**1**)	linear	6.2×10^{-5}	4.1×10^{-10}	62	1.1	this work
[(μ_3-$MoSe_4$)($AgPPh_3$)$_3$(μ_3-Cl)]	cubane	1.1×10^{-4}	5.0×10^{-10}	78	0.8	13a
[(μ_3-WSe_4)($AgPPh_3$)$_3$(μ_3-Cl)]	cubane	1.7×10^{-4}	7.5×10^{-10}	75	0.45	7e
[(μ_3-WSe_4)($AgPCy_3$)$_3$ (μ_3-I)] (**2**)	cubane	2.3×10^{-4}	7.9×10^{-10}	76	0.7	this work
[(μ_3-WSe_4)Ag_3(μ_3-I)(μ-dppm)$_2$] (**4**)	butterfly	6.2×10^{-4}	6.7×10^{-10}	78	0.7	this work
[(μ_3-WSe_4)$_2Ag_4$(μ-dppm)$_3$] (**5**)	hexanuclear	8.9×10^{-4}	1.8×10^{-9}	82	0.4	this work
{[$La(Me_2SO)_8$][(μ-WSe_4)$_3Ag_3$]}$_n$	polymer	2.2×10^{-4}	6.8×10^{-9}	72	0.7	11
[NBu^n_4]$_3$[$WS_4Ag_3Br_4$]	cubane	nd[b]	nd[b]	70	0.6	18c
[NBu^n_4]$_3$[$WS_4Ag_3BrCl_3$]	cubane	nd[b]	nd[b]	70	0.6	18c
[$Mo_2Ag_4S_8(PPh_3)_4$]	cage	1.8×10^{-4}	2.2×10^{-9}	92	0.1	27
[$W_2Ag_4S_8(AsPh_3)_4$]	cage	7.8×10^{-4}	5.9×10^{-10}	92	0.1	30

[a] α_2 is the nonlinear absorption coefficient, and n_2 is the nonlinear refractive index. [b] Not determined.

optical nonlinearity. Since the nonlinear absorption and refraction of the linear trinuclear and cubane tetranuclear heteroselenometallic clusters have been well investigated,[4b,13] the NLO parameters of compounds **1** and **2** with the above respectively structural types were determined with reference to the similar measurement conditions for the comparison, as complied in Table 6. The α_2 and n_2 values for **1** extracted from 7 ns experimental data are 6.2×10^{-5} cm W^{-1} and 4.1×10^{-10} cm^2 W^{-1}, respectively, while the α_2 and n_2 values for **2** under the similar conditions are 2.3×10^{-4} cm W^{-1} and 7.9×10^{-10} cm^2 W^{-1}, respectively.

For the further confirmation of the nonlinear origin and the photostability of the heteroselenometallic clusters with univalent silver atoms, the optical limiting effects of cluster compounds **1**, **2**, **4**, and **5** were also investigated by the pump probe technique.[18b] Figure 9 shows the 7 ns optical limiting experimental results of the samples in CH_2Cl_2 solutions at the same concentration (6.5×10^{-4} M). The probe transmittance is normalized to their linear value. The transmittances of the samples were found to decrease as the laser fluence increases, characteristic of optical limiting.[18b,c] The limiting threshold was defined as the incident fluence, at which the transmittance falls to 65% of the linear transmittance. From Figure 9, the limiting thresholds of compounds **1**, **2**, **4**, and **5** were determined to be ca. 1.1, 0.7, 0.7, and 0.4 J·cm^{-2}, respectively. The saturation fluence transmitted is ~5 J·cm^{-2}.

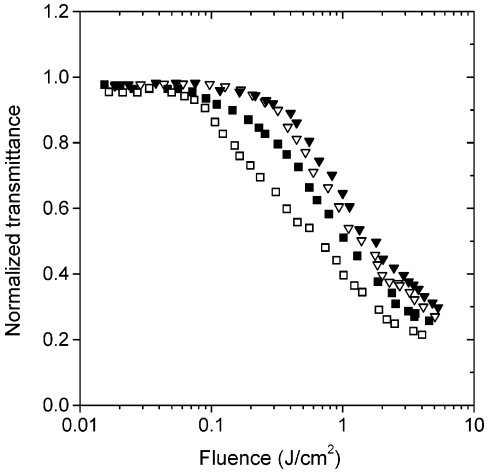

Figure 9. 7 ns optical limiting effect of cluster compounds **1** (solid triangle), **2** (open triangle), **4** (solid square), and **5** (open square), all in 6.5×10^{-4} M in CH_2Cl_2 solution. The energy transmittance is plotted vs the incident fluence.

It should be pointed out that our measurements of the transmitted pulse energy were conducted with the aperture placed in front of the transmission detector. Upon zero time delay, the probe transmittance remains almost unchanged and only begins to decrease after the pump has completely passed away especially in the lower fluence condition.[27] This slow nonlinearity is much more important in the optical performance of the clusters in the 35 ps experiments. Therefore, the maximum transmittance drop is obviously dependent on the pump fluence, and the observed optical limiting behavior for the clusters can be attributed to both nonlinear absorptive and refractive processes. The present four argentoselenometallic compounds were observed to show good photostability. As known, the fluence of the 10 Hz laser pulses is a heat accumulation in the irradiated area, which keeps molecules in this area at high temperature. Cluster molecules with such high temperatures tend to decompose easily, resulting in a lower effective concentration. But the photodegradation becomes a less prominent problem for the four argentoselenometallic compounds during the course of the optical experiments.[13] Further support for the stability of the four cluster samples arises from the fact that the samples remained effective even if the samples were prepared several months before. Several NMR experiments over a period of 2 months showed nearly no change of ^{31}P NMR signal for the samples in solution being determined.

Concluding Remarks

To establish a meaningful structure−NLO property relationship for selenometallic compounds,[28,29] more studies on similar cluster compounds with different compositions with related structures should be carried out. The magnitude of third-order NLO effects is clearly showed if all the sulfur atoms are replaced by selenium atoms in the typical cubanelike clusters.[13] In our previous report, the differences in NLO properties of linear trinuclear cluster compounds containing univalent coinage metals and tetraselenotungstate are attributed to the influence of the skeleton atoms.[4b] It is thus apparent that the NLO absorptive and refractive proper-

(27) Ji, W.; Shi, S.; Du, H. J.; Ge, P.; Tang, S. H.; Xin, X. Q. *J. Phys. Chem.* **1995**, *99*, 17297.
(28) Shi, S.; Lin, Z.; Mo, Y.; Xin, X. Q. *J. Phys. Chem.* **1996**, *100*, 10696.
(29) Shi, S. Nonlinear Optical Properties of Inorganic Clusters. In *Optoelectronic Properties of Inorganic Compounds*; Roundhill, D. M., Fackler, J. P., Jr., Ed.; Plenum Press: New York, 1999; pp 55−105.

ties for linear metal clusters as well as cubanelike clusters are highly sensitive to the heavy atom effect. Therefore, the great potential of transition metal clusters in NLO applications lies in the fact that their NLO properties can be fine-tuned by altering the constituent elements and skeleton structures. In a comparison of the NLO properties of the argentoselenometallic clusters with their sulfur analogues (see Table 3), the following conclusions can be drawn. (1) A structure−NLO property relationship seems to exist in these metal clusters. The cluster compounds with cage structures, such as hexanuclear prism cage $[M_2Ag_4S_8(QPh_3)_4]$[27,30] (M = Mo, W; Q = P, As) and typical cubanelike $[(\mu_3\text{-}WSe_4)(AgPPh_3)_3(\mu_3\text{-}Cl)]$,[7e] show large nonlinear optical properties and optical limiting effects. (2) Heavy atom effect plays an important role in the improvement of the NLO properties of these clusters.[29,31] Introduction of the semiconductor element selenium into metal clusters can effectively improve nonlinear optical absorptive and optical limiting effects of heteroselenometallic compounds in this system. (3) The NLO properties of higher nuclearity metal clusters are usually larger than those of the lower nuclearity analogues. Polynuclearity of heteroselenometallic compounds may thus enhance nonlinear optical absorptive and refractive effects, which will be an approach to design high-nuclear metal cluster materials.[32] (4) Neutral argentoselenometallic compounds supported by σ-donating phosphine ligands were found to exhibit good photostability and relatively stable optical limiting effects, suggesting that this class of clusters is best candidate of optical limiting material among heterometallic clusters studied thus far. To further elucidate the structure−property relationship of metal−selenide-based NLO materials, heteroselenometallic cluster compounds with tailored structures and composition will be designed and synthesized in this laboratory.

Acknowledgment. This project was supported by the Natural Science Foundation of China (Grant 90301005) and the Hong Kong Research Grants Council (Project No. 601506). Q.-F.Z. thanks the Science and Technological Fund of Anhui Province for Outstanding Youth (Grant 06046100) and the Alexander von Humboldt Foundation for the assistance.

Note Added after ASAP Publication. Figures 7 and 8 published ASAP on September 22, 2006 were incorrect. The correct versions were posted on September 26, 2006.

Supporting Information Available: Tables of crystal data, final atomic coordinates, anisotropic thermal parameters, and complete bond lengths and angles for compounds **1**, **2**, **3**·dmf, **4**, and **5**·dmf·CH_2Cl_2 in the paper. This material is available free of charge via the Internet at http://pubs.acs.org.

IC0610839

(30) Sakane, G.; Shibahara, T.; Hou, H. W.; Xin, X. Q.; Shi, S. *Inorg. Chem.* **1995**, *34*, 5363.

(31) (a) Shi, S.; Hou, H. W.; Xin, X. Q. *J. Phys. Chem.* **1995**, *99*, 4050. (b) Ge, P.; Tang, S. H.; Ji, W.; Hou, H. W.; Long, D. L.; Xin, X. Q.; Lu, S. F.; Wu, Q. J. *J. Phys. Chem. B* **1997**, *101*, 27.

(32) (a) Shi, S.; Ji, W.; Xin, X. Q. *J. Phys. Chem.* **1995**, *99*, 894. (b) Niu, Y. Y.; Song, Y. L.; Zheng, H. G.; Xin, X. Q. *New J. Chem.* **2001**, *25*, 945.